1-1-2015

Analytical model of shear behaviour of a fully grouted cable bolt subjected to shearing

Xuwei Li
University of Wollongong, xl866@uowmail.edu.au

Jan Nemcik
University of Wollongong, jnemcik@uow.edu.au

Ali Mirzaghorbanali
University of Wollongong, am001@uowmail.edu.au

Naj Aziz
University of Wollongong, naj@uow.edu.au

Haleh Rasekh
University of Wollongong, hr599@uowmail.edu.au

Analytical model of shear behaviour of a fully grouted cable bolt subjected to shearing

Abstract

A fully grouted cable bolt is normally loaded at rock joints by a combination of the axial and shear forces causing both axial extension and shear deformation of the cable. The proposed analyses presented here attempts to predict the joint shear strength and shear displacement. The analyses are based on the statically indeterminate beam theory and some basic findings and conclusions of other researchers. Parametrical investigation is performed on four influence factors including bolt pretension, joint friction angle, concrete strength and bolt installation angle. Although the true plastic moduli of the cable bolt deflecting section at failure are the essential parameters in this analysis, they are practically impossible to determine. Thus, the average cable moduli obtained from the cable tensile strength tests were used. The proposed analytical model was compared with the experimental results, showing a good agreement. This analytical work aims to develop a simple tool for the practicing geotechnical engineer to effectively evaluate the cable shear behaviour and the influence of fully grouted cable bolts on joint shear resistance.

Disciplines

Engineering | Science and Technology Studies

Publication Details

Li, X., Nemcik, J., Mirzaghorbanali, A., Aziz, N. & Rasekh, H. (2015). Analytical model of shear behaviour of a fully grouted cable bolt subjected to shearing. International Journal of Rock Mechanics and Mining Sciences, 80 31-39.

Analytical model of shear behaviour of a fully grouted cable bolt subjected to shearing

Xuwei Li, Jan Nemcik, Naj Aziz, Ali Mirzaghorbanali, Haleh Rasekh

Faculty of engineering and information science, University of Wollongong, NSW, Australia

Abstract

Cable bolting reinforcement is currently considered to be one of the best methods for improving rock strata conditions and to control the strata movement and deformation. A fully grouted cable bolt is normally loaded at rock joints by a combination of the axial and shear forces causing both axial extension and shear deformation of the cable. The axial and shear loads experienced by cable bolts are very complex as they are influenced by many factors, such as cable strength, cable moduli, cable dimensions, rock strength, and joint properties. The proposed analyses presented here attempt to predict the joint shear strength and shear displacement. The analyses are based on the statically indeterminate beam theory and some basic findings and conclusions of other researchers. The emphasis of this research is to describe the cable contribution to joint shear strength and the cable deflection in the vicinity of rock joint. Parametrical investigation is performed on four influence factors including bolt pretension, joint friction angle, concrete strength and bolt installation angle. Although the true plastic moduli of the cable bolt deflecting section at failure are the essential parameters in this analysis, they are practically impossible to determine. Thus, the average cable moduli obtained from the cable tensile strength tests were used. The proposed analytical model was compared with the experimental results, showing a good agreement. This analytical work aims to develop a simple tool for the practicing geotechnical engineer to effectively evaluate the cable shear behaviour and the influence of fully grouted cable bolts on joint shear resistance.

Keywords: Fully grouted cable bolt, Joint shear strength, Influence factors, Analytical model

1. Introduction

Rock bolting (rebar bolting and cable bolting) is a widely used technique for reinforcing rock masses both in mining and civil engineering projects [1, 2]. Rebar bolt is a single solid steel tendon, while cable bolt is a flexible tendon composed of multi-wire strand which is normally installed and grouted in drilled holes to provide reinforcement in rock masses [3]. The main feature of rock bolting is to reinforce unstable rock strata. Naturally, in

the past attention was given mainly to the tensile behaviour of rebar bolts and cable bolts on the studying of the axial stress distribution in bolts and the load transfer mechanism along the bolt-grout interface. However, a better understanding of the bolt performance in tension and shear is essential to optimise the bolt design and to assess a reinforcing system. This is important for reinforcement of weak or sedimentary rock especially in areas of thinly-laminated strata, high horizontal stress or highly jointed and faulted rock mass.

In recent times, attentions have been given to the lateral interaction between bolts and surrounding rock due to the increasing understanding of the axial load transfer mechanism of rock bolting. Several early publications in 1970's [4-6], 1980's [7-14], and 1990's [2, 15-19] described the shear behaviour of rebar bolts across rock joints. However, during this period, fewer experts devoted themselves on cable bolting. The earliest published tests on the interaction of joints and cable bolts were conducted by Goris [20] as well as Dolinar [21] in 1996, followed by Craig and Aziz [22, 23].

The shear behaviour of cable or rebar bolts and their contribution to joint shear strength is heavily influenced by a number of factors, such as the strength of host material [2, 15, 22, 24, 25], annulus grout thickness [26], axial pretension load [2, 7, 8, 24], grouted or un-grouted bolt [20], bolt installation angle [5, 7, 8, 11, 15, 27, 28], joint roughness coefficient (JRC) [13, 15, 20, 22], loading rate, loading time (creep effect), bolt diameter [15] and cable strength. Some of these factors have been studied in depth, whereas others were rarely analysed. Due to a large number of factors influencing the bolt performance, some of the conclusions in these reported publications contradict each other. For example, in the analysis of the influence of bolt installation angle on bolted joint, Azuar [27], Spang and Egger [15], Ge and Liu [29], and Grasselli [28] pointed out that bolt installation angle clearly influenced the shear strength of bolted joint, whereas Hibino and Motojima [8] stated that the bolt installation angle did not increase the bolted joint shear strength. This may be due to researchers did not always systematically consider the relevant factors influencing the bolt behaviour.

A theoretical model concerning the behaviour of a single grouted cable bolt was developed with consideration of various factors mentioned above. The performance of a cable intersecting a joint was investigated and a theoretical relationship between the axial and lateral load components was mathematically derived. The maximum joint shear resistance and joint shear displacements were determined by combining the cable failure criteria and the loading state derived from structural mechanics analysis.

The effect of all related influencing factors mentioned above were analysed and compared with the existing studies [2, 15]. In addition, this analytical model was also compared with experimental test results to confirm its validity.

2. Mechanical model

When a grouted rebar bolt or cable bolt in rock is subjected to shearing, the bolt deforms and two plastic hinges form at both sides of the joint plane. For the slow rate of loading, reaction forces in the host material (grout and rock) are mobilised and all forces are in equilibrium. Both the bolt and the host material experience the elastic stage and the plastic stage successively.

During loading, the reinforcement bolt and the host material progress from the elastic stage to the plastic stage. In the elastic stage of the host material, the reaction force is roughly proportional to its elastic compression [30, 31]. According to Ferrero's study [2], the shape of the bolt deflecting section can be approximated with a parabolic equation. Thus it is reasonable to assume the reaction force distribution exhibits the same shape in the elastic stage. In the plastic stage of the host material, the reaction force remains constant since the bolt crushes into the host material [32]. Thus a constant uniform distribution of the reaction force is assumed for the plastic stage of the host material.

During shear loading, the bolt moduli decrease from the perfectly elastic state to the fully plastic state along the bolt length, and the reaction force varies from a parabolic distribution to a constant distribution.

According to the analysis of plastic hinge formation, the distance from joint to plastic hinge is normally less than 3~ 4 times the bolt diameter for most commonly used bolts. In Jalalifar's tests [33] on steel rebar bolts, this length was normally less than 60 mm which is less than three times the bolt diameter. In addition, when a bolt deflects due to shearing, the tension and compression loads between bolt and the host material are produced on the top and bottom sides. Since the cohesion between the host material and the bolt is very small, the grout on the tension side can easily detach from the bolt surface. After the grout and rock yields within the compressive zone, the host material is crushed and unable to bear higher compressive load. Based on the above analysis, the frictional effect between the host material and the bolt is negligible as assumed in several previous studies [18, 34].

An assumption is made here that the deflecting section of a bolt between two plastic hinges is statically indeterminate with two fixed ends. Two different mechanical models with elastic reaction and plastic reaction are shown in Fig. 1, respectively.

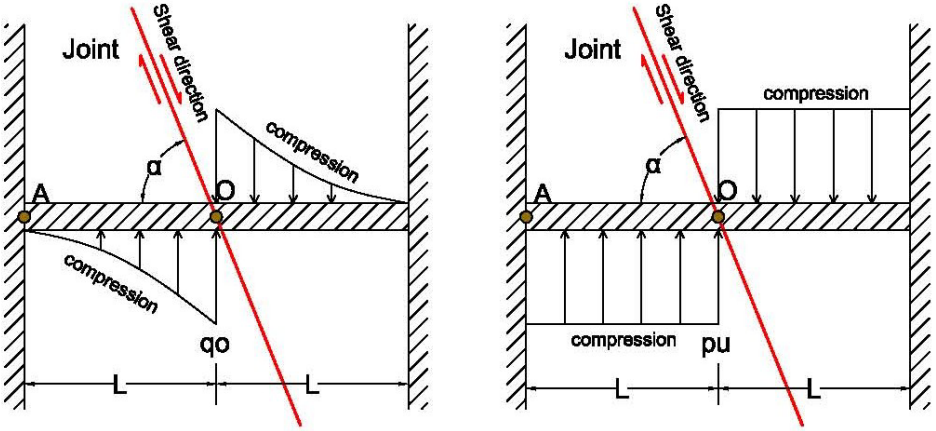

Fig. 1. Simplified mechanical models of a tendon subjected to shearing both in elastic and plastic subgrade

3. Bolt contribution to joint shear strength

There have been various analytical and experimental investigations undertaken looking at the cable and rebar bolts and their contribution to joint shear strength. These studies suggest that two types of contribution, the frictional effect and the dowel effect, are made by a bolt to the joint shear strength. Fig. 2 shows the typical loading state of a bolt-reinforced joint.

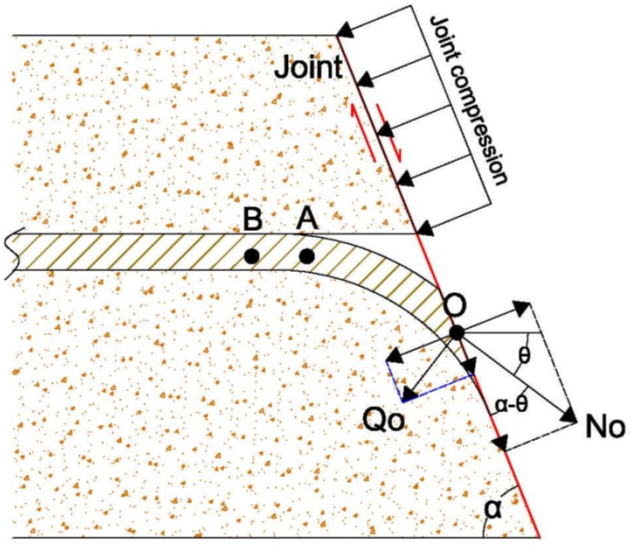

Fig. 2. Loads induced on joint and in bolt

The bolt contribution to joint shear strength is:

$$R = N_o \cos(\alpha - \theta) + Q_o \sin(\alpha - \theta) + [N_o \sin(\alpha - \theta) - Q_o \cos(\alpha - \theta)]tan\emptyset \quad (1)$$

Where R is the bolt contribution to joint shear strength; N_o, Q_o are the tensile and shear force components of a bolt at the bolt-joint intersection, respectively; α is the bolt installation angle to the joint; θ is the deflection angle (bending) of bolt.

There are two different dowel effects. One is related to the combination of the parallel components of the axial and shear forces of the bolt to the joint [18, 28, 33], and the expression is:

$$R_{dowel} = N_o \cos(\alpha - \theta) + Q_o \sin(\alpha - \theta) \quad (2)$$

The other one is connected to only the bolt shear force itself, including the normal component and the parallel component of the bolt shear force to the joint which produce indirect and direct contribution respectively to the joint shear strength [2]. The expression is:

$$R_{dowel} = Q_o \sin(\alpha - \theta) - Q_o \cos(\alpha - \theta)\, tan\emptyset \quad (3)$$

In this paper, the direct contribution of both the axial and shear forces is considered as the dowel effect, thus the first expression, Eq. (2), was used.

4. Theoretical analysis

4.1 Elastic stage of the host material

To solve a statically indeterminate beam problem, first one needs to transform the original problem into a statically determinate beam by removing all redundant reactions [35]. In this problem, there are three redundant reactions that can be removed. Considering half of the beam, a combination of axial force R_1, shear force R_2, and bending moment R_3 can be used to represent the restraint of the other half as shown in Fig. 3.

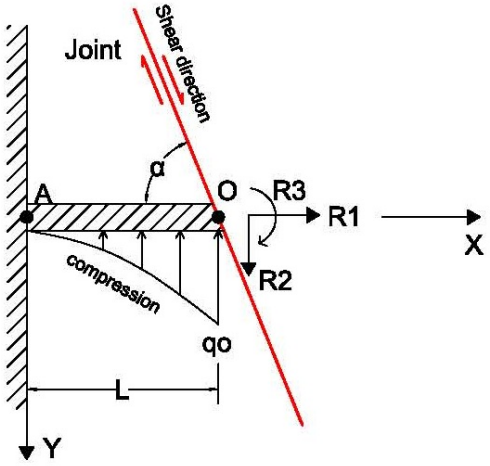

Fig. 3. Loading state of a statically determinate beam

Thus, based on the force method of statically indeterminate structures, three compatibility equations can be written:

$$\begin{cases} f_{11}R_1 + f_{12}R_2 + f_{13}R_3 + \Delta_{1q} = \Delta_1 \\ f_{21}R_1 + f_{22}R_2 + f_{23}R_3 + \Delta_{2q} = \Delta_2 \\ f_{31}R_1 + f_{32}R_2 + f_{33}R_3 + \Delta_{3q} = \Delta_3 \end{cases} \quad (4)$$

Or in a matrix form,

$$\begin{bmatrix} f_{11} & f_{12} & f_{13} \\ f_{21} & f_{22} & f_{23} \\ f_{31} & f_{32} & f_{33} \end{bmatrix} \begin{bmatrix} R_1 \\ R_2 \\ R_3 \end{bmatrix} + \begin{bmatrix} \Delta_{1q} \\ \Delta_{2q} \\ \Delta_{3q} \end{bmatrix} = \begin{bmatrix} \Delta_1 \\ \Delta_2 \\ \Delta_3 \end{bmatrix} \quad (5)$$

Or simply

$$\boldsymbol{fR} + \Delta_{\boldsymbol{q}} = \Delta \quad (6)$$

Where f_{ij} is the displacement along the direction of R_i caused by the unit of R_j, also known as flexibility coefficient; Δ_{iq} is the displacement along the R_i direction caused by the grout reaction force; Δ_i, $i = 1,2,3$, is the axial extension, the lateral deflection and the cable deflection angle at point O.

According to the loading state in the elastic stage, the influence of the grout reaction force is:

$$q(x) = \frac{q_o}{L^2} x^2 \quad (7)$$

$$Q(x) = \frac{q_o}{3L^2} x^3 \quad (8)$$

$$M(x) = \frac{q_o}{12L^2} x^4 \quad (9)$$

$$v(x) = \frac{1}{EI} \cdot \frac{q_o}{360L^2} x^6 \quad (10)$$

Thus, the flexibility matrix and the deformation matrix induced by external loads can be obtained based on beam theory as:

$$\boldsymbol{f} = \begin{bmatrix} \frac{L}{EA} & 0 & 0 \\ 0 & \frac{L^3}{3EI} + \frac{kL}{GA} & \frac{L^2}{2EI} \\ 0 & \frac{L^2}{2EI} & \frac{L}{EI} \end{bmatrix} \quad (11)$$

$$\Delta_q = \begin{bmatrix} 0 \\ -\left(\frac{q_o L^4}{360EI} + \frac{k q_o L^2}{12GA}\right) \\ -\frac{q_o L^3}{60EI} \end{bmatrix} \quad (12)$$

Where L is the plastic hinge distance from the joint to hinges, approximately equal to $\sqrt{\frac{\pi d^3 \sigma_{yield} - 4N_A d}{16 p_u}}$ [34] (p_u,the maximum concrete reaction); A and I are the area and the inertia moment of the tendon cross section, respectively; $E$and G are, respectively, the tensile and shear modulus of the tendon; q_o is the compression load density at point O; k is a concentration coefficient of the shear stress distribution at the tendon cross section, which is equal to 4/3 for a solid cross section and is determined using the inner and outer radius for a hollow cross section [36].

Because of the deflecting beam symmetry, it is reasonable to assume that $R_3 = 0$ [17]. Thus, substituting Eqs. (11) and (12) into Eq. (5) yields:

$$\begin{bmatrix} \frac{L}{EA}R_1 \\ \left(\frac{L^3}{3EI}+\frac{kL}{GA}\right)R_2-\left(\frac{q_oL^4}{360EI}+\frac{kq_oL^2}{12GA}\right) \\ \frac{L^2}{2EI}R_2-\frac{q_oL^3}{60EI} \end{bmatrix} = \begin{bmatrix} \Delta_1 \\ \Delta_2 \\ \Delta_3 \end{bmatrix} \tag{13}$$

Solving Eq. (13) in reference to Δ produces:

$$R_1 = \frac{EA}{L}\Delta_1 \tag{14}$$

$$R_2 = \frac{\left(2GAEIL^2+60kE^2I^2\right)\Delta_3-12GAEIL\Delta_2}{18EIkL^2-3GAL^4} \tag{15}$$

$$q_o = \frac{\left(80GAEIL^2+240kE^2I^2\right)\Delta_3-120GAEIL\Delta_2}{6EIkL^3-GAL^5} \tag{16}$$

Based on Eq. (8), the shear force at point O can be obtained:

$$R_2 = \frac{q_oL}{3} \tag{17}$$

Combining Eqs. (15), (16) and (17) gives the relationship between $\Delta_2$and Δ_3:

$$\Delta_3 = \frac{18GAL}{13GAL^2+30kEI}\cdot\Delta_2 \tag{18}$$

Substituting Eq. (18) into (15) and (16) yields:

$$R_2 = \frac{240kGAE^2I^2-40G^2A^2EIL^2}{(6EIkL-GAL^3)(13GAL^2+30kEI)}\cdot\Delta_2 \tag{19}$$

$$q_o = \frac{720kGAE^2I^2-120G^2A^2EIL^2}{(6EIkL^2-GAL^4)(13GAL^2+30kEI)}\cdot\Delta_2 \tag{20}$$

According to the deformation relationship shown in Fig. 4, the following equation exists:

$$\frac{\Delta_2}{\Delta_1} = \frac{sin\alpha}{\cos(\alpha-\theta)} = \frac{sin\alpha}{\cos\alpha\cos\theta+\sin\alpha\sin\theta} \tag{21}$$

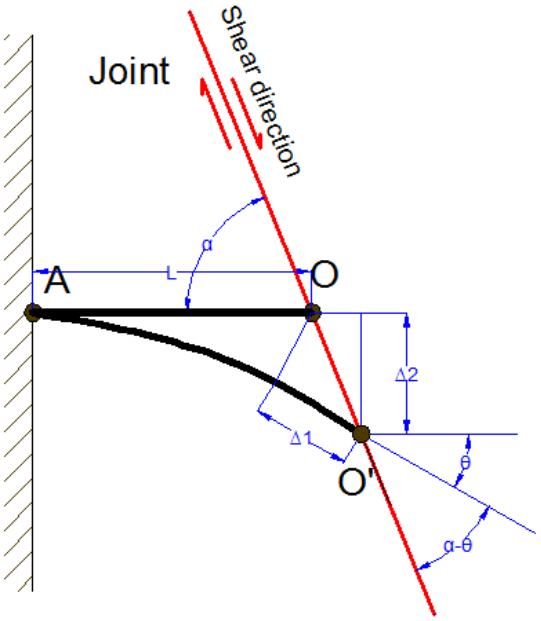

Fig. 4. Deformation compatibility condition at bolt-joint intersection

Since θ, equal to Δ_3, is very small in elastic stage, one can get:

$$\Delta_1 = \frac{\cos\alpha + \sin\alpha \cdot \Delta_3}{sin\alpha} \cdot \Delta_2 \quad (22)$$

For the yield at the maximum bending moment point A, due to a combination of the axial load and bending moment, the following expressions are used [16, 32, 37]:

$$\frac{N_A}{A} + \frac{M_A y}{I} = \sigma_{yield} \quad (23)$$

$$\left(\frac{N_A}{N_{yield}}\right)^2 + \left(\frac{M_A}{M_{pl}}\right)^2 = 1 \quad (24)$$

Where N_{yield}, is the tensile yield limit of a tendon, equal to $A\sigma_{yield}$ and M_{pl}, is the plastic bending moment, equal to $\frac{1.69\pi d^3}{32}\sigma_{yield}$. Note that, Eqs. (23) and (24) correspond to the start of yielding at the cable outmost layer and the formation of a fully plasticized cross section, respectively.

Thus combining Eqs. (14), (19), (20) and (22), the tendon loading state with the increase of the shear displacement can be obtained and then the occurrence of the plastic hinges formation in the elastic stage can be checked using Eqs. (23) and (24). To further simplify these calculations, it is sufficient to only check the state with the load density (q_o) being equal to the maximum concrete reaction (p_u, equal to $\sigma_c d$[16]).

4.2 Plastic stage of the host material

When the shear deformation of a grouted tendon increases, the host medium reaction increases as well. The host medium plasticisation starts after the reaction force exceeds its

yield strength. And from then on, the reaction force in the plastic zone remains constant. Thus a new loading state appears as shown in Fig. 5.

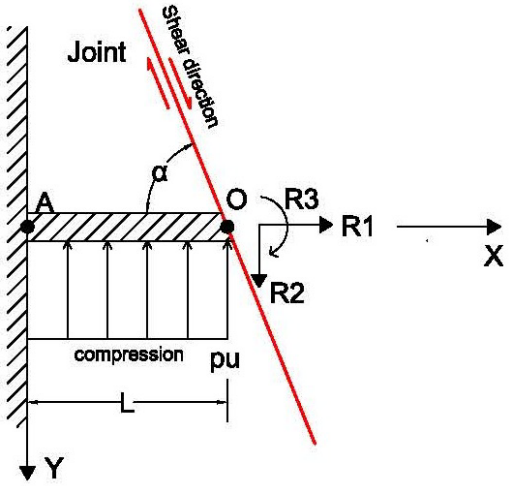

Fig. 5. Loading state of a statically determinate beam

The elastic stage in the host medium transforms into the plastic stage in a plasticization process. In this process plasticisation in the host medium propagates from the joint surface inwards to the plastic hinges. Finally, the whole length between the joint surface and plastic hinges behaves in the plastic manner. In this study, this transition stage is not considered.

In the similar manner as in the elastic stage, the redundant reactions can be written as follows:

$$R_1 = \frac{EA}{L}\Delta_1 \tag{25}$$

$$R_2 = \frac{\Delta_2+\frac{p_u L^4}{8EI}+\frac{kp_u L^2}{2GA}}{\frac{L^3}{3EI}+\frac{KL}{GA}} \tag{26}$$

$$R_2 = \frac{\Delta_3+\frac{p_u L^3}{6EI}}{\frac{L^2}{2EI}} \tag{27}$$

Since the deflection angle in the elastic stage is very small, in the plastic stage the deflection angle is assumed to start from zero. Thus the deformation compatibility relation in the plastic stage is the same as in the elastic stage.

$$k_1 = \frac{\Delta_2}{\Delta_1} = \frac{sin\alpha}{\cos(\alpha-\theta)} \tag{28}$$

Combining Eqs. (25), (26) and (28) produces:

$$R_1 = k_2 \cdot R_2 + k_3 \tag{29}$$

Where:

$$k_2 = \frac{\frac{AL^2}{3I}+\frac{kE}{G}}{k_1}$$

$$k_3 = -\frac{\frac{p_u AL^2}{8I} + \frac{kp_u EL}{2G}}{k_1}$$

When the axial force and shear force at point O (Fig. 5) satisfy the failure criteria (Eq. (30)) [10, 18, 24], then the cable breaks. Thus, the axial and shear forces at point O when the cable failure occurs can be obtained from Eqs. (29) and (30).

$$\left(\frac{N_o}{N_f}\right)^2 + \left(\frac{Q_o}{Q_f}\right)^2 = 1 \tag{30}$$

Where N_f, is the ultimate tensile strength of a tendon, equal to $A\sigma_f$ and Q_f, is the ultimate shear strength of a tendon, equal to $A\tau_f$; When τ_f is equal to $\frac{\sigma_f}{2}$, this equation represents the Tresca criterion in plane stress state. When τ_f is equal to $\frac{\sigma_f}{\sqrt{3}}$, this equation becomes the Von Mises criterion in plane stress state. In the following analysis, the Tresca criterion is to be used in this paper.

After obtaining the axial and shear forces at point O, substituting them into Eq. (1) yields the bolt/tendon contribution to joint shear strength.

4.3 Joint shear displacement

The final deformation curve of a tendon at failure subjected to shearing consists of two parts, the host medium reaction and the tendon shear force. With the shear force (Q_o) derived from Eqs. (29) and (30), and the host medium reaction strength (p_u) [16], the corresponding contributions can be described as follow:

$$V_{Q_o} = \frac{Q_o}{6EI}(3Lx^2 - x^3) + \frac{kQ_o}{GA}x \tag{31}$$

$$V_{p_u} = \frac{p_u}{24EI}(x^4 - 4Lx^3 - 4L^2x^2) + \frac{kp_u}{2GA}x^2 \tag{32}$$

Then, the actual deformation curve at failure is given by:

$$V(x) = V_{Q_o} - V_{p_u} \tag{33}$$

For the case when $x = L$, the bolt shear displacement ($V(L)$) at point O is equal to one half of the total joint shear displacement since Eq. (33) represents a half space only (see Fig. 1).

5. Parametrical investigation

In the derivation of the bolt contribution to joint shear strength, a variety of related factors are taken into account. All these factors together determine the bolt performance subjected to shearing. Accordingly in view of cable bolts, four of these factors are

investigated in detail, including bolt pretension, joint friction angle, concrete strength (the host medium), and bolt installation angle.

5.1 Bolt pretension

Pretension is an important influence factor in a cable-reinforced jointed concrete system. Many variables are influenced by pretension during shearing, such as the plastic hinge distance, the ultimate shear failure displacement, the shear and axial forces at failure. Thus the cable bolt contribution to joint shear strength is also impacted. In simple terms, the greater the cable bolt pretension, the smaller the plastic hinge distance and the ultimate (final) shear displacement. Though the influence of cable bolt pretension on some variables is clear, its impact on the joint shear resistance capacity is not apparent since these variables can also influence each other.

Fig. 6 shows the relationship between the shear and axial forces at different cable pretensions, and a specific cable failure case ($E = 4GPa$, $G = 1.6GP$). The other parameters involved in this section are $\emptyset = 24°$, $d = 0.022m$. Solutions for other cases are listed in Table 1 to Table 3.

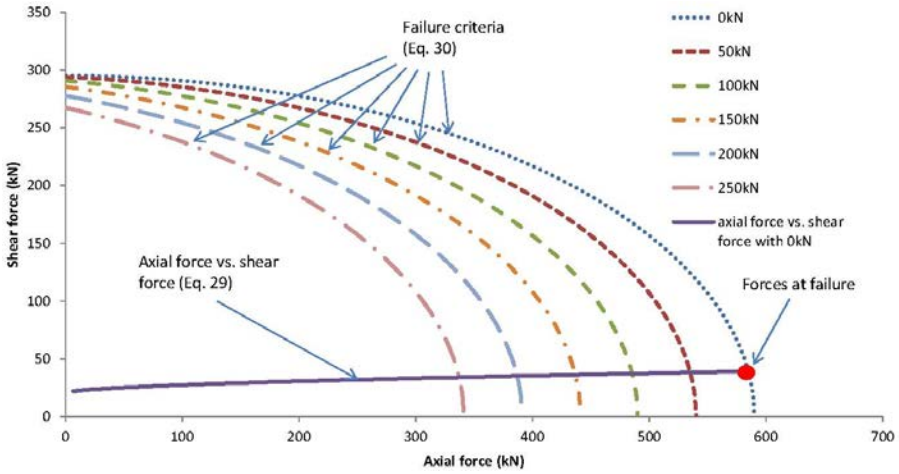

Fig. 6. Shear force vs. axial force in the cable

Table 1 Cable bolt contribution to joint shear strength at varied cable pretensions

Pretension effect (E=2GPa G=0.8GPa)						
Pretension (kN)	0	50	100	150	200	250
θ (radian)	1.54	1.41	1.296	1.184	1.08	0.98
No (kN)	587	586	588	587	587	587
Qo (kN)	35.7	34.8	34.2	33.5	33.0	32.6
R_{No} (kN)	595	620	636	641	639	631
R_{Qo} (kN)	-15	-10	-5	-1	3	6
R (kN)	580	610	631	640	642	638

Table 2 Cable bolt contribution to joint shear strength at varied cable pretensions

Pretension effect ($E_{average}$=4GPa $G_{average}$=1.6GPa)						
Pretension (kN)	0	50	100	150	200	250
θ (radian)	0.929	0.873	0.818	0.760	0.705	0.646
No (kN)	587	584	585	582	586	586
Qo (kN)	39.3	39.0	38.7	38.5	38.5	38.5
R_{No} (kN)	625	613	603	587	576	559
R_{Qo} (kN)	10	12	14	16	18	21
R (kN)	634	625	617	603	594	579

Table 3 Cable bolt contribution to joint shear strength at varied cable pretensions

Pretension effect (E=10GPa G=4GPa)						
Pretension (kN)	0	50	100	150	200	250
θ (radian)	0.544	0.516	0.486	0.456	0.424	0.389
No (kN)	581	584	582	583	583	581
Qo (kN)	49.0	49.3	49.5	49.9	50.3	50.8
R_{No} (kN)	519	512	498	487	474	457
R_{Qo} (kN)	31	32	34	35	37	39
R (kN)	550	544	532	522	510	495

Theoretically, when cable bolt failure occurs at the bolt-joint intersection, the entire cable deflecting section between the plastic hinges should be plastic. Thus the cable plastic stage moduli should be used in the calculation. During the cable strain hardening, cable moduli vary from the maximum to a minimum. Fig. 7 shows a typical stress-strain relationship of a single straight smooth cable wire loaded in tension. From the laboratory tensile tests carried out on cable wires [38], the averages of cable wire's plastic moduli are $E = 4GPa$, $G = 1.6GPa$. In these analyses, a range of cable's plastic moduli are used in Tables 1, 2 and 3.

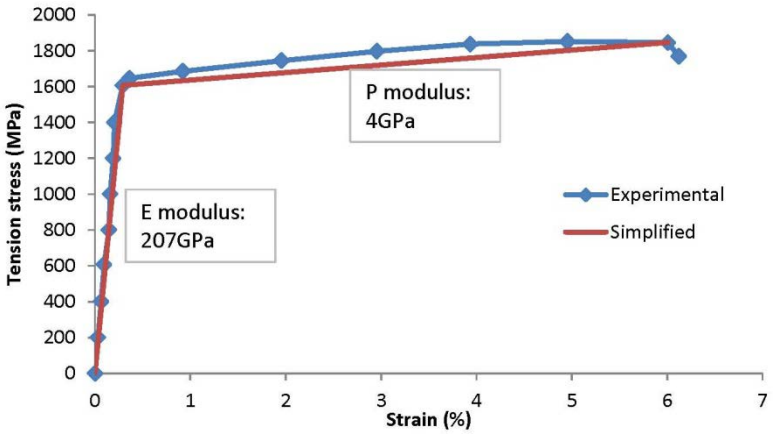

Fig. 7. Stress strain relationship of a single straight smooth cable wire

From Tables 1, 2 and 3 it can be seen that the cable pretension has two different effects on the joint shear strength. For a cable failing at the smaller moduli, the greater the cable

pretension, the more contribution the cable makes. In contrast, an exactly opposite trend takes place for a cable failing at the average or higher moduli.

Fig. 8 shows the double shear test results of SUMO cables and the testing apparatus. This figure offers the shear displacement and shear force at failure and the average shear stiffness of the shear system rather than real loading-displacement curves. Details about the testing procedure can be found in existing publications [23, 24, 26, 33, 34]. Compared with the experimental results shown in Fig. 8, it is clear that the cable pretension effect in this analysis is consistent with the experimental tests. Specifically, the cable pretension decreased the shear strength of joints reinforced with indented SUMO cables which normally failed at much smaller shear displacements than the plain cable. This corresponds to the cable pretension effect shown in Table 2 and Table 3. However, the cable pretension increased the shear strength of joints strengthened with plain SUMO cables which normally failed at much larger shear displacements. And thus this corresponds to the cable pretension effect shown in Table 1.

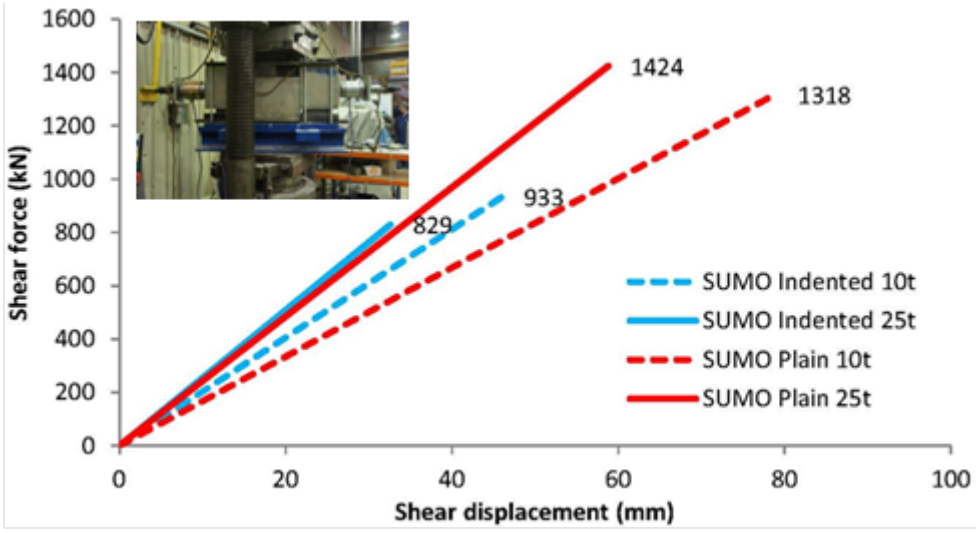

Fig. 8. Pretension effect on joint shear resistance capacity

In the above analysis, there are two different cable pretension effects on the bolted joint shear strength. Going back to check the cable contribution to joint shear strength described in Eq. (1), since the bolt installation angle and the joint friction angle are constant the cable contribution was found to be influenced by two parameters, the cable loading state (the axial force and shear force) and the cable deflection angle. Therefore, theoretically the cable pretension affects the joint shear strength by changing these two parameters. Checking data in Tables 1, 2 and 3, it can be clearly seen that both the axial and shear forces obtained at varied cable pretensions do scarcely vary. Thus the joint shear strength variation is mainly due to the

cable deflection angle. Since the cable pretension has two different effects, the cable deflection angle should correspondingly have two effects on the joint shear strength as well.

There is a maximum joint shear strength point (turning point) when the cable deflection angle changes. In Tables 1 to 3, the joint shear strength increases with the increase of deflection angle when the cable deflection angle is less than approximately one radian (57°) and decreases when the deflection angle exceeds one radian. Therefore one radian is the turning point of the cable pretension effect on joint shear strength.

Why is it one radian? Is it always one radian for all cases or just a special case? Since the joint shear strength is ultimately determined by the cable loading state and the friction angle (Eq. (1)), the turning point of cable deflection angle (where the maximum shear capacity occurs) should be determined by them as well.

Figs. 9 and 10 show the influences of the axial load and joint friction coefficient respectively on the turning point of cable deflection angle for a perpendicularly reinforced joint.

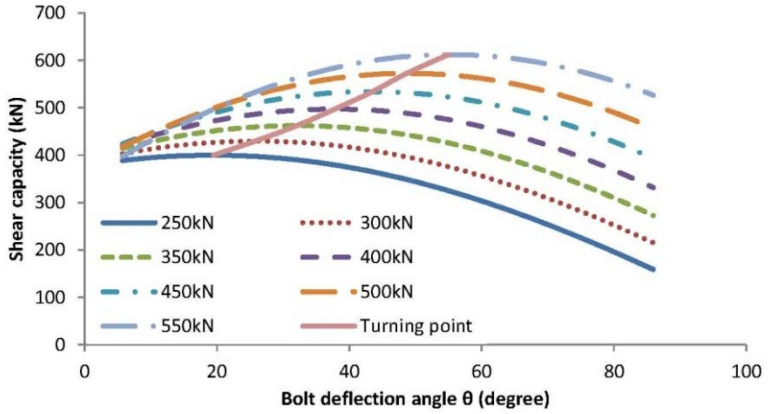

Fig. 9. Influence of the axial load at failure on the turning point of joint shear strength with the joint friction coefficient of 0.44.

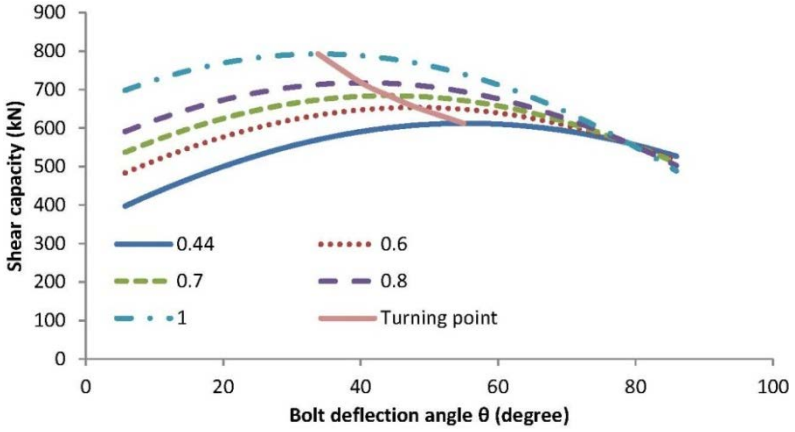

Fig. 10. Influence of the joint friction coefficient on the turning point of shear strength with the axial load of 550kN

In Fig. 9, the turning point has a very clear increasing trend with the increase in axial load. The turning point increases from 19° to 55° with the axial load ascending from 250kN to 550kN. However, in Fig. 10, the turning point decreases with the increase of friction angle. While the turning point is located at 55° with a friction coefficient of 0.44, it drops to only about 34° with a friction coefficient of 1. So the turning point of deflection angle is not fixed and it changes with the variation of the cable loading state and the joint friction angle. The calculated cable deflection turning point of one radian in Tables 1 to 3 is for a specific case ($tan\emptyset = 0.44, \alpha = 90°, N_o \approx 580kN$).

5.2 Joint friction angle

Since the joint friction angle appeared only in the calculation of cable contribution to joint shear strength (Eq. (1)), it only affects the joint shear strength but not the final loading state of cable bolts at failure. The influence of the joint friction angle has been given in Fig. 10 and its effect on the turning point of the cable deflection angle has been discussed as well. In addition to this, the joint friction angle effect on joint shear strength weakens with the increase of the deflection angle and there is almost no difference when the deflection angle approaches 80° as shown in Fig. 10 and Fig. 11. The large deflection angle normally occurs in the case of weak concrete and small pretension. And thus the joint friction angle effect is much more evident in the opposite situation (strong concrete and large pretension) (Fig. 11). Also as expected, higher friction angle produces higher joint shear strength.

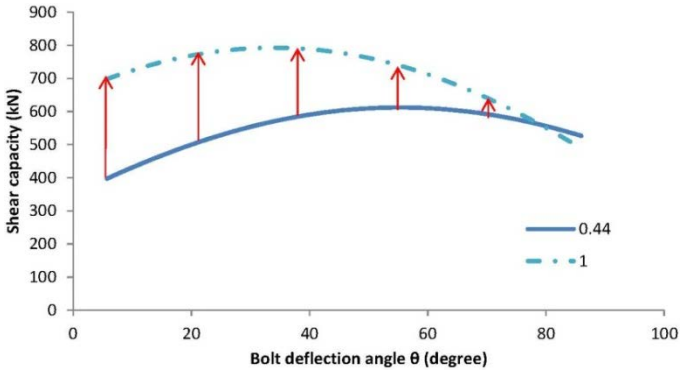

Fig. 11. Influence of the joint friction coefficient on the joint shear strength with varied deflection angle for the axial load of 550kN

5.3 Concrete strength

The strength of concrete and grout material has a significant influence on the cable bolt deformation and the reinforced joint shear strength [2, 15, 22, 24, 25]. It is reasonable to make an assumption that the shear displacement increases with the decrease of concrete

strength. Studies[24, 25] carried out by researchers also support this assumption. Thus it is also credible that the tensile strain of cable bolts anchored in soft concrete progresses further than in hard concrete. Hence, the cable moduli at failure are assumed to increase with the increasing concrete strength (Table 4). The theoretically calculated results of cable bolts installed in concrete of varied strengths are given in Table 4.

Table 4 Variation of the cable loading state at failure with varied concrete strength

Concrete strength (MPa)	Joint shear failure load per joint (kN)	Cable modulus at failure (GPa)	Joint shear displacement (mm)	Axial force component at bolt-joint intersection (kN)	Shear force component at bolt-joint intersection (kN)
20	641	3	119	588	23
40	631	4	73	584	39
60	611	5	53	579	56
80	592	6	42	572	72

Similar to the experimental tests carried out by other researchers[2, 15], the weaker the concrete, the larger the shear strength of cabled joints. The shear displacement is very large when the concrete is very soft, but it cannot further increase since the concrete will collapse prior to cable failure. When the concrete is very strong, the failure will be similar to a guillotine test since the shear force will increase and the axial force will decrease. The calculated values in Table 4 indicate that as the concrete strength increases the cable bolt shear force increases at a greater rate than the decrease in axial force. This is consistent with that more tensile failures of bolts were observed in weak concrete while more tensile-shear combined failures were seen in hard concrete [2].

5.4 Bolt installation angle

In practical application, cable bolts may be anchored at any angle to joints and therefore for each case they will behave differently. Experimental conclusions have been drawn in several papers by other researchers[5, 7, 8, 11, 15, 27, 28]. In their studies, the bolt installation angle across the joint was found to influence the bolt failure mode, the shear strength and the deformation stiffness of a bolted joint.

The influence of bolt installation angle on the joint shear strength is analysed here based on the proposed method and shown in Fig. 12. The relevant parameters are $E = 4GPa$, $G = 1.6GPa$, $d = 0.022m$, $\sigma_{yield} = 1677MPa$, $\sigma_f = 1885MPa$. Clearly, the bolt installation angle influences joint shear strength magnitudes which are further modified by the joint friction angle as shown in Fig. 12. Under above given conditions, for the extreme

case of the joint friction coefficient of 0, the joint shear strength continuously decreases with the increase of bolt installation angle, whereas for a friction coefficient of 0.8, the joint shear strength continues to increase. The case of high joint friction angle partly agrees with Spang and Egger's conclusions[15]. For the friction angle between these two cases, the joint shear strength increases for lower installation angles, reaching maximum and then decreases. This maximum versus the bolt installation angle is described by the "turning point" line shown in Fig. 12. So there is a maximum joint shear strength point for each joint friction angle, and a turning point of bolt installation angle. For practical purposes it can be assumed that in most cases the rock joint coefficient of friction would be higher than approximately 0.4. So we can infer that the maximum joint shear strength will occur mostly within the bolt installation angle of 70°-90° (Fig. 12).

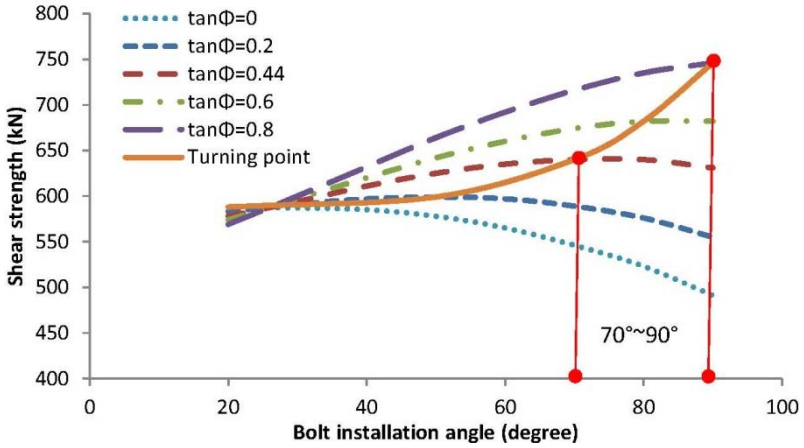

Fig. 12. Influence of bolt installation angle on the joint shear strength with varied joint friction coefficients

6. Comparison of analytical and experimental results

To validate this proposed analytical method, the results were compared to the double shear experiments carried out on commonly used cables tested at the University of Wollongong laboratory.

To compare the proposed model with the double shear experimental study, same dimensions and required parameters were used for calculations. Parameters include the diameter of cable, the yield and failure strength of cable, the compressive strength of concrete, the cable installation angle to joint, the friction angle of joint, the tensile and shear modulus of the deformed cable bolt section at failure. Although one could get the cable moduli for both the elastic and plastic stages from the laboratory tests, it appeared to be impossible to accurately predict the average moduli of the cable section between plastic hinges at failure when subjected to shearing. And this is because the cable moduli vary during the shearing

process from the initial elastic state to the final plastic state. In addition, a cable may snap earlier due to special factors contributing to cable or concrete weakness. Yet, without these weaknesses, the cable assembly will continue to yield until failure. The specific moduli for each cable are determined by the degree of cable plasticisation at failure. It is reasonable to assume that for a constant plastic hinge length, the larger the joint shear displacement, the smaller the cable moduli. So to predict the joint shear resistance and shear displacement at failure, one can apply larger moduli to cables failing normally at smaller shear displacements and smaller moduli to cables failing at larger shear displacements. However, it is still not easy to specify suitable cable moduli to an individual specific condition since the shear displacement is affected by many factors.

To validate the proposed model, cable moduli at failure were determined according to the actual shear displacements obtained in experiments. The joint shear capacities of the analytical method and the experimental tests were then compared. Cable bolts used in laboratory double shear tests are shown in Fig. 13. Fig. 14 illustrates the shear resistance comparison of different cables tested at varied pretensions obtained from both the analytical model and experiments. Table 5 lists the specific moduli of each test calculated according to actual joint shear displacements and Eq. (33).

Fig. 13. Cable bolts tested in double shear tests

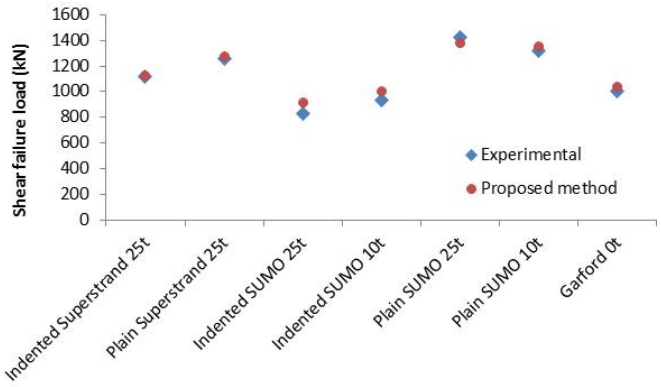

Fig. 14. Reinforced joint shear resistance obtained from the experimental tests and computed with the proposed analytical method

Table 5 Moduli calculated according to actual shear displacements

Cable type	Pretension(t)	E(GPa)	Joint shear displacement(mm)	Concrete strength(MPa)
Indented Superstrand	25	1.3	74.3	36
Plain Superstrand	25	2	65.2	41
Indented SUMO	25	15	32.6	32
Indented SUMO	10	12	46	42
Plain SUMO	25	2	58.8	41
Plain SUMO	10	2	78.9	43
Plain Garford	0	2	82	42

All indented cable bolts listed in this table may also be called spirally ribbed cable bolts by some manufactures.

In Fig. 14, it is obvious that the analytical model agrees closely with experimental test results where the derived moduli were based on actual joint shear displacements. Specifically, the differences between the experimental results and analytical model are small and not more than 11%. Thus the proposed method is acceptable from the view of predicting the shear strength with experimentally obtained joint shear displacements.

It is seen from Table 5 that the moduli of the cable plastic hinge section at failure are in close relationship with their surface profiles. Except for the indented Superstrand 25t cable, all other indented cables showed larger moduli than the plain cables. This indicates the feasibility of determining cable moduli based on the cable strand surface profile. The smaller moduli of the indented Superstrand 25t cable obtained due to its bigger shear displacement seem unreasonable when compared with its plain counterpart. The reason of this behaviour may be that the weaker concrete allowed more shear displacement, leading to its late failure and smaller moduli (Table 5). Unlike the strand surface profile effect, the pretension effect on the cable moduli is not very noticeable.

7. Conclusions and Recommendations

Based on the statically indeterminate beam theory an analytical model that enables realistic predictions of the cable bolted joint shear strength and shear displacement is developed. This model was compared with experimental tests, showing close agreement.

In addition, parametric investigations were performed about four main influence factors including concrete strength, cable pretension, joint friction angle and bolt installation angle and conclusions were drawn as follows:

- Cable pretension affects the bolted joint shear strength in two different ways. This effect is mainly decided by the plastic moduli of the cable deflecting section at cable failure.
- The joint friction angle affects the bolted joint shear capacity. This effect diminishes with increase in cable deflection angle and tapers off when the cable deflection angle approaches 80°.
- Hard concrete/rock provides lower joint shear strength and smaller joint shear displacements.
- The effect of bolt installation angle on joint shear strength is affected by the joint friction angle. The maximum joint shear strength will occur mostly within the bolt installation angle ranging 70°-90° in practical joint conditions.

However, it should be noted that the proposed model was based on idealized assumptions, thus there were some limitations. For example, the joint friction coefficient was considered as constant, but actually it might change during shearing process due to the joint surface damage. The distribution of reaction force of the host material was assumed to comply with the parabolic equation and to remain constant in the elastic stage and the plastic stage of the host material, respectively. However, they did not exactly comply with the assumed distributions due to the heterogeneity of the concrete.

Acknowledgements

The first author would like to thank the China Scholarship Council (CSC) and the University of Wollongong for funding his study in Australia. The authors wish to thank the university personnel who assisted to complete the double shear tests conducted at the University of Wollongong, especially the laboratory technicians Colin Devenish, Alan Grant, Cameron Neilson, Hooman Ghojavand and David Gilbert. This research is funded by organizations including Jennmar Australia and Orica. Constructive suggestions from anonymous reviewers are also acknowledged.

References

[1] Windsor CR. Rock reinforcement systems. Int J Rock Mech Min Sci. 1997;34:919-51.

[2] Ferrero AM. The shear strength of reinforced rock joints. Int J Rock Mech Min Sci. 1995;32:595-605.

[3] Hutchinson DJ, Diederichs MS. Cablebolting in underground mines: BiTech Publishers; 1996.

[4] Dulacka H. Dowel action of reinforcing crossing cracks in concrete. ACIJ. 1972:754-7.

[5] Bjurstrom S. Shear strength of hard rock joint reinforced by grouted untensioned bolts. International Congress of Rock Mechanics. Denver1974. p. 1194-9.

[6] Fuller PG, Cox RHT. Rock reinforcement design based on control of joint displacement - a new concept. Australia Tunnelling Congress. Sydney1978. p. 28-35.

[7] Haas CJ. Analysis of rock bolting to prevent shear movement in fractured ground. Journal of Mining Engineering. 1981:698-704.

[8] Hibino S, Motojima M. Effects of rock bolting in jointed rocks. International Sympsium of Weak Rock. Tokyo1981. p. 1052-62.

[9] Dight PM. A case study of the behaviour of a rock slope reinforced with fully grouted rock bolts. Int Symp Rock bolting. Abisko1982. p. 523-38.

[10] Dight PM. Improvements to the Stability of Rock Walls in Open Pit Mines [Ph.D. Thesis]. Melbourne: Monash University; 1983.

[11] Egger P, Fernandes H. A novel triaxial press - study of achored jointed models. International Congress on Rock Mechanics. Melbourne1983. p. 171-5.

[12] Ludvig B. Shear tests on rock bolts. Int Symp Rock Bolting. Abisko1983. p. 193-203.

[13] Stillborg S. Experimental investigation of steel cables for rock reinforcement in hard rock [Ph.D. Thesis]. Lulea: Lulea University of Technology; 1984.

[14] Aydan O. The stabilisation of rock engineering structures by rockbolts [Ph.D. Thesis]. Nagoya: Nagoya University; 1989.

[15] Spang K, Egger P. Action of fully-grouted bolts in jointed rock and factors of influence. Rock Mech Rock Eng. 1990;23:201-29.

[16] Pellet F. Strength and deformability of jointed rock masses reinforced by rock bolts [Ph.D. Thesis]. Lausane: EPFL; 1994.

[17] Pellet F, Egger P, Fernandes H. Contribution of fully bonded rock bolts to the shear strength of joints: analytical and experimental evaluation. International Conference on Mechanics of Jointed and Faulted Rock1995.

[18] Pellet F, Egger P. Analytical model for the mechanical behaviour of bolted rock joints subjected to shearing. International Journal of Rock Mechanics and Rock Engineering. 1996:73-97.

[19] Kharchafi M, Grasselli G, Egger P. 3D behaviour of bolted rock joints: experimental and numerical study. Symposium of Mechanics of Jointed and Faulted Rock1999. p. 299-304.

[20] Goris JM, Martin LA, Curtin RP. Shear behaviour of cable bolt supports in horizontal bedded deposits. CIM Bull. 1996;89:124-8.

[21] Dolinar DR, Tadolini SC, Blackwell DV. High horizontal movements in longwall gate roads controlled by cable support systems. International Conference on Ground Control in Mining. Morgantown1996. p. 497-509.

[22] Craig P, Aziz N. Shear testing of 28mm hollow strand TG cable bolt. In: Aziz P, editor. Coal Operators' Conference Wollongong, NSW, Australia2010. p. 171-9.

[23] Aziz N, Kay H, Nemcik J, Stefan M. Shear strength properties of Hilti plain and indented strand cable bolts. In: Naj A, editor. Coal Operators' Conference. Wollongong, NSW, Australia2014. p. 156-62.

[24] Jalalifar H, Aziz N, Hadi M. The effect of surface profile, rock strength and pretension load on bending behaviour of fully grouted bolts. Geotechnical and Geological Engineering. 2006;24:1203-27.
[25] Aziz N, Damian P, Richard W. Double shear testing of bolts. In: Naj A, editor. Coal Operators' Conference. Wollongong, NSW, AUstralia2003.
[26] Aziz N, Jalalifar H, Hadi M. The effect of resin thickness on bolt-grout-concrete interaction in shear. In: Naj A, editor. Coal 2005: coal operators' conference. Wollongong2005. p. 3-9.
[27] Azuar JJ. Stabilization de massifs rocheux fissures par barres dacier scellees. 1977.
[28] Grasselli G. 3D behaviour of bolted rock joints: experimental and numerical study. Int J Rock Mech Min Sci. 2005;42:13-24.
[29] Ge X, Liu J. Study on the shear Resistance Behaviour of Bolted Rock Joints [J]. Chinese Jounal of Geotechnical Engineering. 1988;1:001.
[30] Lambe TW, Whitman RV. Soil mechanics SI version: John Wiley & Sons; 2008.
[31] Terzaghi K. Evalution of conefficients of subgrade reaction. Geotechnique. 1955;5:297-326.
[32] Holmberg M, Stille H. The mechanical behaviour of a single grouted bolt. International Symposium on Rock Support. Rotterdam1992. p. 473-81.
[33] Jalalifar H, Aziz N. Experimental and 3D numerical simulation of reinforced shear joints. Rock Mech Rock Eng. 2010;43:95-103.
[34] Jalalifar H. A new approach in determining the load transfer mechanism in fully grouted bolts [Ph.D. Thesis]. Wollongong: University of Wollongong; 2006.
[35] Hibbeler RC, Tan K-H, Nolan B. Structural analysis: Pearson Prentice Hall; 2006.
[36] Gere JM, Timoshenko SP. Mechanics of materials: KENT Publishing Company, Elsevier Science BV, Amsterdam; 1990.
[37] Neal BG. The plastic methods of structural analysis. New York: John Wiley & Sons; 1977.
[38] Orica. Mechanical property test report. Orica; 2014.